CHAPTER 126

VERTICAL VARIABILITY OF COASTAL SEDIMENT TRANSPORT

Ryszard B. Zeidler*

ABSTRACT

The semiempirical theory of turbulent diffusion may be used as a mathematical tool for description of suspended sediment mechanics. The Author's solutions, with their exponential vertical profiles of sediment concentration, are presented in various ranges of time, space, and external factors. The inherent concept of eddy diffusivity K is shown to be ambiguous and incoherent. Therefore it is purposeless to investigate thoroughly the vertical profiles and other details of K. Accordingly, the Author makes use of his own and alien laboratory and field findings to propose such estimates of K under r e g u l a r waves and currents which are not continuous functions of the vertical coordinate but instead are locally averaged over depth layers. These estimates become more complex in real coastal zones due to the randomness of waves and currents, wave breaking, three-dimensionality and nonstationarity of nearbed turbulence, a variety of interactions, and other sources of sediment dispersion. Hence g r o s s estimates of averaged K seem even more appropriate; some formulae are put forward. The vertical profiles of sediment concentration are presented herein along with examples of sediment transport rates measured in nearshore zones.

1. SUSPENDED SEDIMENT IN TERMS OF DIFFUSION THEORIES

1.1. Analytical Solutions

The concentration of suspended sediment, C, in an unsteady two-dimensional flow with velocity u_0 may be described by the equation of turbulent diffusion

$$\frac{\partial C}{\partial t} + u_0(x,y)\frac{\partial C}{\partial x} = K_{01}(y)\frac{\partial^2 C}{\partial x^2} + \frac{\partial}{\partial y}\left(K_{02}(y)\frac{\partial C}{\partial y}\right) + w_s\frac{\partial C}{\partial y}\cdots \qquad (1)$$

in which

* Professor, Polish Academy of Sciences' Institute of Hydro-Engineering (IBW PAN), 7 Kościerska, 80-953 Gdańsk

K_{01}, K_{02} = eddy diffusivities
w_s = settling velocity
t = time.

The system of coordinates is shown in Fig. 1 where the initial and boundary conditions are outlined for the two problems distinguished, A and B.

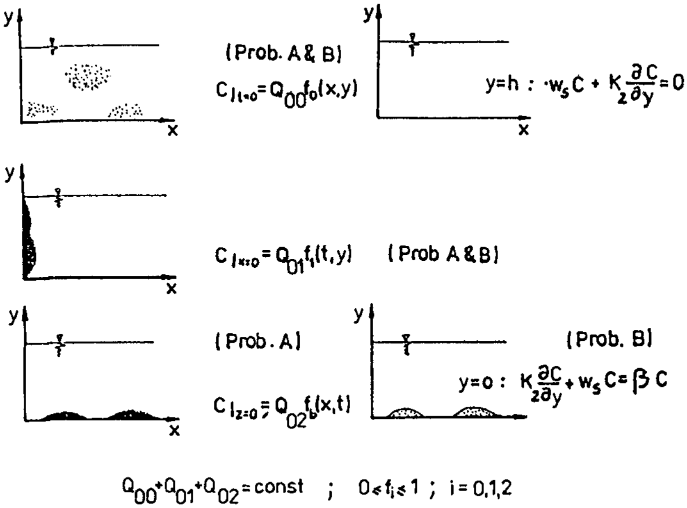

Fig. 1 Initial and Boundary Conditions

Eq. 1 in dimensionless form reads

$$\frac{\partial C^*}{\partial t^*} + 2au^*(x^*,y^*)\frac{\partial C^*}{\partial x^*} = \alpha_1^*(y^*)\frac{\partial^2 C^*}{\partial x^{*2}} + \alpha_2^*(y^*)\frac{\partial^2 C^*}{\partial y^{*2}} + (2b + \alpha_2^{*\prime}(y^*))\frac{\partial C^*}{\partial y^*} \quad (2)$$

in which

$$u_0 = Uu^*(x,y); \qquad 0 \le u^*(x,y) \le 1$$
$$K_{01} = K_1\alpha_1^*(y); \qquad 0 \le \alpha_1^*(y) \le 1$$
$$K_{02} = K_{02}\alpha_2^*(y); \qquad 0 \le \alpha_2^*(y) \le 1$$
$$a = \frac{U \cdot h}{2\sqrt{K_1 \cdot K_2}}; \qquad b = \frac{w_s h}{2K_2}; \qquad C^* = \frac{C}{Q_{02}};$$
$$x^* = \sqrt{\frac{K_2}{K_1}}\frac{x}{h}; \qquad y^* = \frac{y}{h}; \qquad t^* = \frac{K_2}{h^2}t$$

The asterisks will be neglected henceforth.

Eq. 2 has been solved for the so-called problem A_0, with constant coefficients, and subsequently envelopes have been found for other versions of the problems A and B (Nguyen and Zeidler, 1982). The solution was obtained as polynomial series, by methods of integral transforms. It assumes the form

$$C(x,y,t) = C_1(x,y) + C_2(x,y,t) + Q_0\left[C_3(y,t) + C_4(x,y,t)\right] + \\ + Q_1\left[C_5(x,y) - C_6(x,y,t)\right] \qquad (3)$$

in which each of the six terms $C_1 \cdots C_6$ is linked to specific initial and boundary conditions, and $Q_0 = Q_{00}/Q_{02}$, $Q_1 = Q_{01}/Q_{02}$.

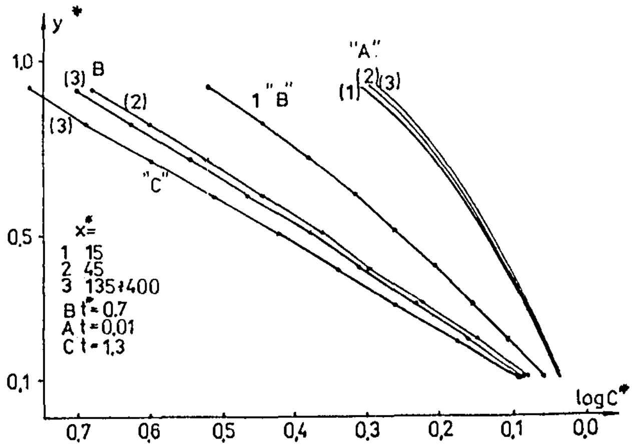

Fig. 2 Examples of Numerical Solutions to Problem A_0

The numerical results depicted in Fig. 2 make it easy to analyse Eq. 3. In the tested intervals of dimensionless $15 \le x^* \le 400$, $0.01 \le t^* \le 1.3$ one may see that the initial convex-up C-profiles, for $t^* = 0.1$, gradually transform into linear (in the semilog plot), for the longest time $t^* = 1.3$. Hence the concentration profiles in stabilized conditions (long $x \to X$ and $t \to T$) of the problem A_0 are exponential, as emphasized in Fig. 3a. Analysis of solutions to the other problems A and B (Nguyen and Zeidler, 1982) shows that they are contained within certain limits C^- and C^+, as presented in Fig. 3b.

1.2. Experimental Evidence

It is appropriate to verify how Eq. 3 agrees with laboratory and field data. The vertical profiles of C have been checked as to their character, numerical values of the exponent b, and temporal variation. Longitudinal variation, $C(x)$, has been

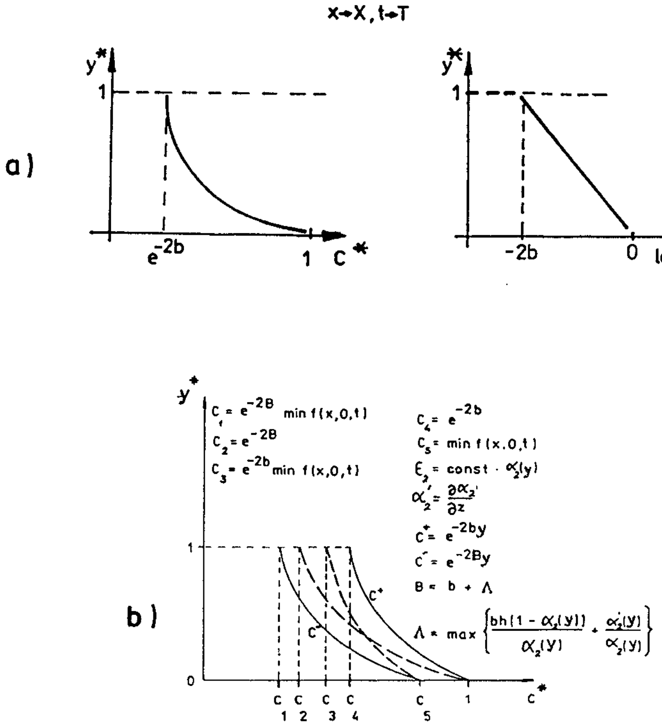

Fig. 3 Equilibrium Solutions to Problem A_0 (top) and to Problem A (bottom)

investigated, along with the effect of sand mixtures and other features. Several alien and three Polish sets of data, each embodying extensive series of C, have been employed, and many additional can be found in bibliographical sources. Some typical examples are presented below.

The numerous data utilized confirm the theoretical exponential vertical profile $C(y)$, with the following important modification. In the semilogarithmic plot, such as the one in Fig. 3a (right), the straight line is almost always replaced by two or three straight lines, in two or three layers: near-bed, central, and near-surface. The two lower layers are pronounced i.a. in the sets measured by Taggart et al (1972), who however adhered to the power-type profile, with corrections proposed by A. T. Ippen. Fig. 4 shows that the exponential representation is much more natural if only the layered structure is accepted.

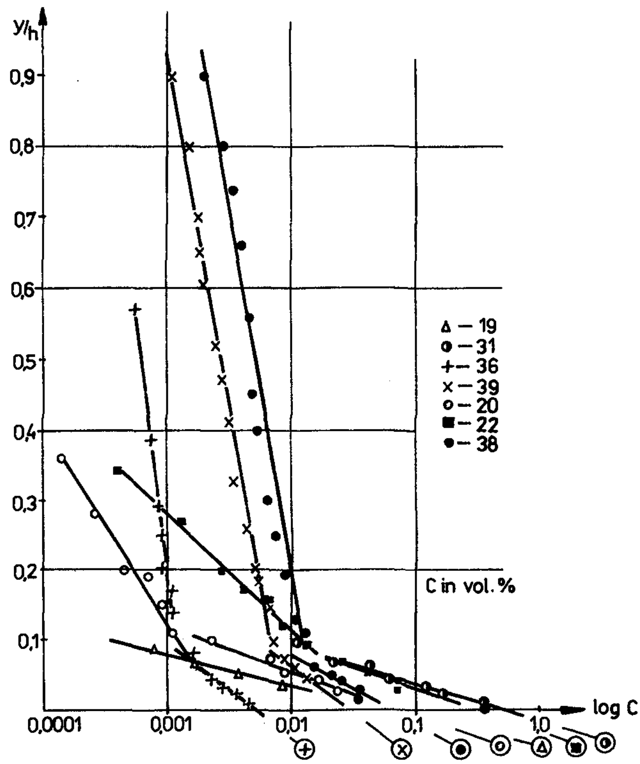

Fig. 4 Sediment Concentration Measured by Taggart et al (1972) in Runs 19...38

The theoretical exponent b agrees well with the experimental data if one assumes $b \simeq 5\frac{w_*}{u_*}$ near bed or $b \simeq 2.5\frac{w_*}{u_*}$ in the central layer; in which u_* = shear velocity. These figures are substantiated in Ch. 2.

One may postulate a few causes of the layered configuration of $C(z)$, such as sediment grading and the associated vertical variability of the von Karman constant.

However, the most important argument is due to the eddy diffusivity $K_y(y) \equiv K_{02}(y)$. It may be inferred that details of the variation of $K_y(y)$ are not essential and that a certain layer-averaged $\overline{K}_y$ is sufficient to describe the basic features of $C(y)$, cf. Fig. 5. Further comments are provided in Ch. 2.

Numerous experimental data show that the layered exponential C-profiles are characteristic not only for flows but also under waves, cf. Skafel and Krishnappan

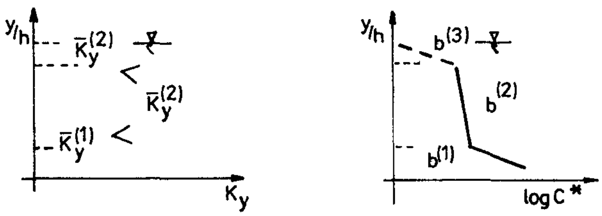

Fig. 5 Correspondence of Exponent b and Layer-Averaged $\overline{K}_y$

(1984), Antsyferov and Kosyan (1986) and many others. Some of the Author's results are presented in Ch. 3. It is also worth noting that such C-profiles are generated by different turbulence mechanisms, i.e. nearbed shear and friction, wave oscillations, wave breaking etc. Hence one may conclude that gross estimates of K, or its equivalents, provide better representation of complex coastal phenomena than detailed fields $K(y)$. These estimates are discussed in Ch. 3. The following arguments in Sec. 2.1 prove how ambiguous the detailed $K(...)$ could be.

2. EDDY DIFFUSIVITY IN THE COASTAL ZONE

2.1. Concept of Eddy Viscosity

The Reynolds equations read

$$\rho \frac{d\mathbf{u}}{dt} = \rho \mathrm{F} - \operatorname{grad} p + \mu \Delta \mathbf{u} + \operatorname{div} \Pi \tag{4}$$

in which

$\mathbf{u} = iu_x + ju_y + ku_z =$ velocity
F = external mass forces
p, ρ = pressure and density, respectively
μ = dynamic coefficient of molecular viscosity,

while the Reynolds tensor Π is

$$\Pi = \begin{bmatrix} -\rho\overline{u_x'^2} & -\rho\overline{u_x'u_y'} & -\rho\overline{u_x'u_z'} \\ -\rho\overline{u_x'u_y'} & -\rho\overline{u_y'^2} & -\rho\overline{u_y'u_z'} \\ -\rho\overline{u_x'u_z'} & -\rho\overline{u_y'u_z'} & -\rho\overline{u_z'^2} \end{bmatrix} \tag{5}$$

One may distinguish diffusion theories, in which Π is coupled with the mean strain rate tensor S, and "differential" models, with expanded equations for Π. Let us dwell on the diffusion theory, and consider a few cases

1. Scalar eddy viscosity, homogeneous constitutive equation

$$\Pi_{ij} = \mu_T S_{ij} \tag{6}$$

The following defects are inherent

(a) For $S_{ij} \to 0$ (and $\mathbf{u} \neq 0$) one obtains $\Pi_{ij} \to 0$, which does not explain the occurrence of Π_{ij} in isotopic turbulence

(b) Each component of Π_{ij} depends on one component of S_{ij}, in disagreement with observations, e.g. spatial structure of turbulence in 1-D flows

(c) Traces of both sides in Eq. 6 disagree, i.e. $tr\Pi = -2\rho k < 0$

$$\mathrm{tr}(\mu_T S) = \begin{cases} \mu_T \mathrm{div}\mathbf{u} = 0 & \text{for } \rho = \text{const} \\ \mu_T \mathrm{div}\mathbf{u} = -\dfrac{\mu_T}{\rho}\dfrac{d\rho}{dt} \gtrless & \text{for } \rho \neq \text{const} \end{cases} \tag{7}$$

(d) By definition, Π_{ii} is not greater than zero, while it can be positive by Eq. 6.

2. Eddy viscosity is a 2-nd rank tensor; homogeneous constitutive equation

$$\Pi_{ij} = \mu_{Tik} S_{jk} \tag{8}$$

or

$$\Pi_{xx} = \mu_{Txx}S_{xx} + \mu_{Txy}S_{xy} + \mu_{Txz}S_{xz};\ \Pi_{xy} = \mu_{Txx}S_{yx} + \mu_{Txy}S_{yy} + \mu_{Txz}S_{yz} \cdots \text{etc.}$$

The following defects surface:

(a) cf. (a) under (1)

(b) tr Π should be < 0 (see (c) under (1)) while from Eq. 8 one has tr $\Pi = \mu_{Tij}S_{ij} \gtrless 0$

(c) For 1-D flow one obtains $\Pi_{zz} = \Pi_{zy} = \Pi_{yz} = 0$, in contradiction with experiments

(d) Π components in Eq. 8 are asymmetric, in contrast to Eq. 5

(e) cf. (d) under (1)

3. Eddy viscosity is a 2-nd rank tensor; inhomogeneous & composite constitutive equation

$$\Pi_{ij} = -2\rho\alpha_{ij}k + \frac{1}{2}(\mu_{Til}S_{lj} + \mu_{Tjl}S_{li}) \tag{9}$$

in which

$$\alpha_{ij} \begin{cases} =0 & \text{for} \quad i \neq j \\ \neq 0 & \text{for} \quad i = j \end{cases}$$

The following defects persist

(a) incomplete set of constitutive variables

(b) LHS & RHS traces of Eq. 9 are not necessarily equal

(c) diagonal Π_{ii} can be positive in Eq. 9

(d) cf. (b) under (1)

(e) α must satisfy $\alpha_{ij} = \alpha E_{ij}$; otherwise α_{ij} is not a tensor

(f) a new quantity, k, turbulence energy enters and must be found, so that the defects of the "differential models" are taken over.

More assumptions can be proposed, such as a 4-th rank tensor for μ_T and inhomogeneous constitutive equations etc. (Sawicki, 1988). Some corrections of the above schemes are likely but, for all possible versions, it must be concluded that the concept of eddy viscosity, and its theoretical implementation are, by and large, incoherent and vulnerable.

In addition, one must remember that eddy viscosity is not identical with eddy diffusivity

$$\mathrm{K} = \beta\mu_T\,, \qquad \text{with} \qquad \beta \neq 1 \tag{10}$$

Hence, although the concepts of eddy viscosity and eddy diffusivity are widely used, it is better to apply them with caution, and restrict oneself to gross estimates.

2.2. Formulae for K; the Coastal Zone

Our primary finding in Ch. 1 may be summarized in the following dimensional triad

$$C \sim \exp(-2b\frac{y}{h}); \quad b = \frac{w_s h}{2K_y}; \quad \text{const } K_y \text{ in } 2\cdots 3 \text{ layers} \tag{11}$$

One may make use of Prandtl's suggestion

$$K = \text{const}\, B(U_{\max} - U_{\min}) \tag{12}$$

in which

B = width of mixing zone

$U_{\max}, U_{\min}$ = maximum and minimum velocity in the mixing zone, respectively.

One may also endeavour

$$K_y = \text{const} u_* \times h \tag{13}$$

in which u_* = shear velocity.

For open-channel flow Elder gave const $\equiv 0.23$, which in our case would yield

$$2b = 4.35\frac{w_s}{u_*} \tag{14}$$

The search for a functional form of K can be more elaborate (Yaglom, 1976). Assume $\beta = 1$ and

$$K_{ij} = \begin{cases} \mu/\rho k_{ij}(\frac{\rho u_* y}{\mu}) & \text{for} \quad y_+ = \frac{\rho y u_*}{\mu} > 0 \\ \kappa_{ij} u_* y & \text{for} \quad y_+ \gg 1 \end{cases} \tag{15}$$

in which

$\kappa_{yy} \equiv \kappa_1 = \frac{\kappa}{Pr_t} \to 0.45 \cdots 0.48$

κ, Pr_t = von Karman and Prandtl coefficient, respectively

k_{ij}= dimensionless quantity.

On the other hand, the classical arguments of linear shear stress profile and logarithmic velocity profile lead to the parabolic K;

$$K_y = \kappa u_* y(1 - y/h) \tag{16}$$

Equations 15 and 16 may be compromised:

$$K_y = \begin{cases} 0.9\kappa u_* h(1 - \frac{y}{h}) \\ \kappa u_* y(1 - \frac{y}{h}) \\ \kappa, u_* y \end{cases} \quad \text{for} \quad y = \begin{cases} 0.85 \cdots 1.0h \\ 0.15 \cdots 0.85h \\ 0 \cdots 0.15h \end{cases} \tag{17}$$

Fig. 6 shows the above K_y together with respective values of $2b$ averaged in the three layers. The experimental data reviewed in this study, yielding $\frac{\overline{2b}}{w_s/u_*}$ about 10 near bed and 5 in the central layer (see Ch. 1) agree well with the analysis outlined in Fig. 6

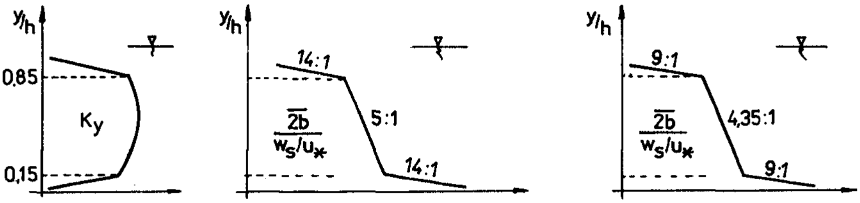

Fig. 6 Theoretically Postulated Values of b

Now examine the most common situations in the coastal zone. For waves (tilde), currents (overbar), long waves ($\wedge$) and turbulence (prime) one has

$$\mathrm{u} = \bar{\mathrm{u}} + \hat{\mathrm{u}} + \tilde{\mathrm{u}} + \mathrm{u}' \tag{18.1}$$

$$C = \bar{C} + \hat{C} + \tilde{C} + C' \tag{18.2}$$

Substituted into the diffusion equation

$$\frac{\partial C}{\partial t} + \frac{\partial u_i C}{\partial x_i} + w_s \frac{\partial C}{\partial y} + Q_c = 0 \tag{19}$$

with the source term Q_c, the components of Eq. 18 produce

$$(\frac{\partial}{\partial x_i})\ \overline{uC} = \overline{uC} + \overline{\hat{u}\hat{C}} + \overline{\tilde{u}\tilde{C}} + \overline{u'C'} \tag{20}$$

the cross-terms being uncorrelated.
One usually assumes

$$\overline{\tilde{u}\tilde{C}} = -\tilde{K}\frac{\partial \bar{C}}{\partial y}; \quad \overline{u'c'} = K\frac{\partial \bar{C}}{\partial y} \tag{21}$$

Stive and Wind (1985) neglected $\overline{u'C'} \ll \tilde{u}\tilde{C}$, which might be unjustified, as the available data shows.

Various formulae have been proposed for $\tilde{K}$ and K, e.g. Homma and Horikawa (1962) (1965), Kennedy and Locher (1972), Skafel and Krishnappan (1984), Antsyferov and Kosyan (1986). A certain insight into the possible structure of $\tilde{K}$, K... is provided by the Author's data on coastal dispersion (Sec. 2.3).

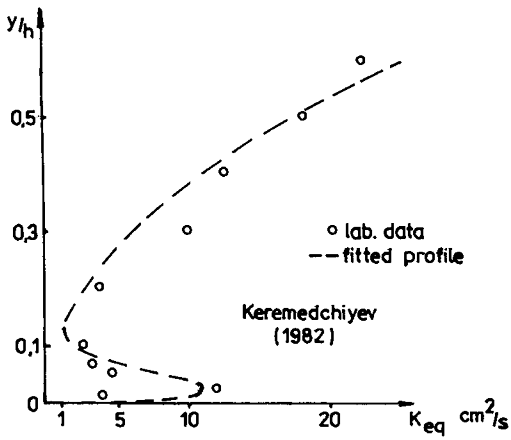

Fig. 7 Eddy Diffusivity Measured in Laboratory

It appears that the fluxes $\rho\ \overline{\tilde{u}\tilde{C}}$ and $\rho\ \overline{u}'\overline{C}'$, i.e. $\tilde{K}$ and K, respectively, are diversified over depth, which is signalled in Fig. 7, with the dominance of K, due to bottom turbulence, in the nearbed layer and $\tilde{K}$, due to wave-induced mixing in the central layer.

2.3. Laboratory and Field Investigations of Eddy Diffusivity

The Author carried out two extensive studies on the dispersion of passive matter. One of them has dealt with regular waves, in a laboratory flume, and the other was conducted in the field where random waves and turbulence dominated the dispersion.

In the wave flume, naturally buoyant particles were ejected at selected segments of bed ripples, and their movements were tracked with a high-speed camera. By this means the following Lagrangian properties of the nearbed layer could be obtained in various wave phases:

$$\overline{\mathbf{Y}(\tau)} = \int_{t_0}^{t_0+\tau} \overline{\mathbf{V}(\mathrm{x}, t)}dt; \tag{22.1}$$

$$\mathbf{Y}'(\tau) = \mathbf{Y}(\tau) - \overline{\mathbf{Y}(\tau)} = \int_{t_0}^{t_0+\tau} \mathbf{V}'(\mathrm{x}, t)dt \tag{22.2}$$

$$D_{ij}(\tau) = \overline{\mathbf{Y}_i'(\tau)\mathbf{Y}_j'(\tau)} = \int_{t_0}^{t_0+\tau}\int_{t_0}^{t_0+\tau} \overline{\mathbf{V}_i'(\mathrm{x}_1 t_1)\mathbf{V}_j'(\mathrm{x}_1 t_2)}dt_1 dt_2 =$$

$$= \iint_{t_0}^{t_0+\tau} B_i j(t_1,\, t_2)dt_1 dt_2 \tag{22.3}$$

Since the study is described elsewhere (Zeidler, 1972), we shall not dwell on the theory and some secondary aspects reported, such as spectra, but merely confine ourselves to the most relevant findings on the tensors of displacements $\mathbf{Y}$ and velocities $\mathbf{V}$, that is D_{ij} and B_{ij}, respectively. The examples given in Fig. 8 depict the complexity of dispersion, even in these seemingly simple regular wave conditions. The vertical profiles of dispersion vary considerably over wave period (Fig. 8a), while the average dispersion after longer times (Fig. 8b) displays certain features of homogeneous turbulence. The Lagrangian velocity tensor B_{ij} also depends on a wave phase (Fig. 8c).

The field studies embodied simultaneous measurements of waves, water velocities and sediment concentration, the latter with a radioisotopic probe, in a vertical profile with smoothly moving instrumentation. The emission noise of the radioactivity source, Am-241, was filtered out, and all signals were processed to obtain correlational and spectral characteristics. The following results can be singled out for the frequency range $0.2 \mathrel{\tilde{<}} f \mathrel{\tilde{<}} 2\,cps$, which may be attributed to random surface waves.

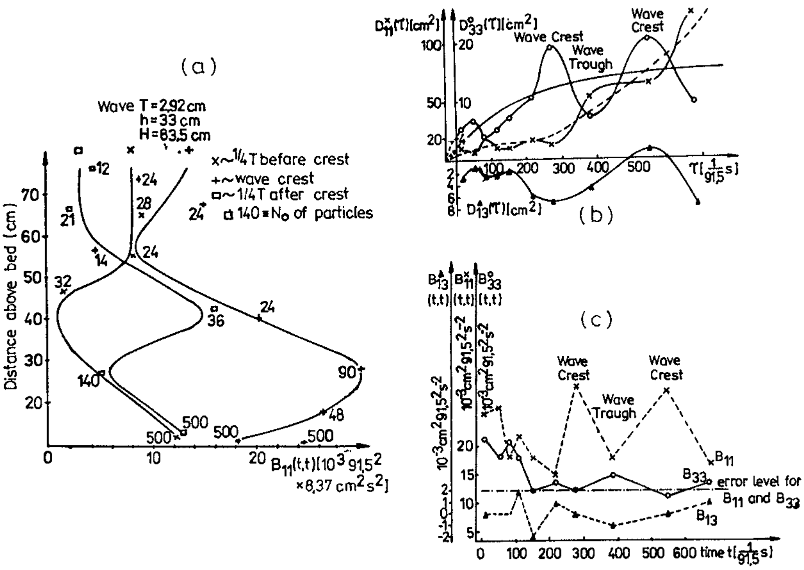

Fig. 8 Lagrangian Velocity Correlation Moments B_{ij} Across Depth (a) and in Time Domain (c) and Displacement Correlation Moments D_{ij} (b)

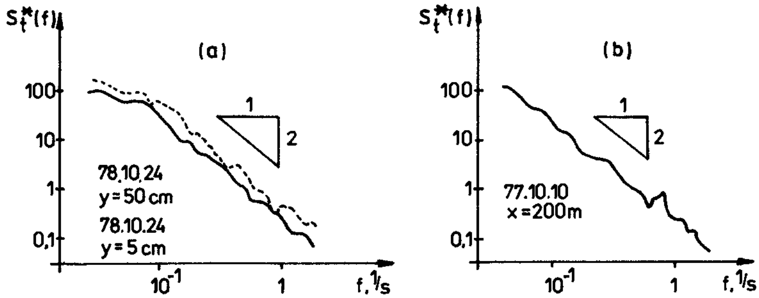

Fig. 9 Shear-Dominated Spectra of Sediment Concentration (a) and Fluorescent Dye (b) Measured in Field

Fluctuations of cross-shore water velocity, $u' \equiv u'_x$ are correlated best with surface waves, while fluctuations of the longshore velocity, $v' \equiv u'_y$, can be linked to shear flow. Fluctuations of sediment concentration measured have been found roughly analogous to concentration fluctuations of fluorescent tracers, which is illustrated in Fig. 9 showing spectra for the two kinds of passive coastal matter, i.e. suspended sediment (left) and a neutrally-buoyant tracer (right). Hence, fluorescent tracer studies may be utilized in sedimentation problems. It appears that in the situations covered, with random waves recorded in twenty-odd cycles, C' series were controlled strongly by bed shear near bottom and were dominated by waves at the free surface. The correlations $\overline{C'v'}$ are of important order of magnitude (Fig. 10). More research is however needed on both sediment concentration and turbulence. Inter alia, wave breaking still remains poorly explored as a very important source of turbulence.

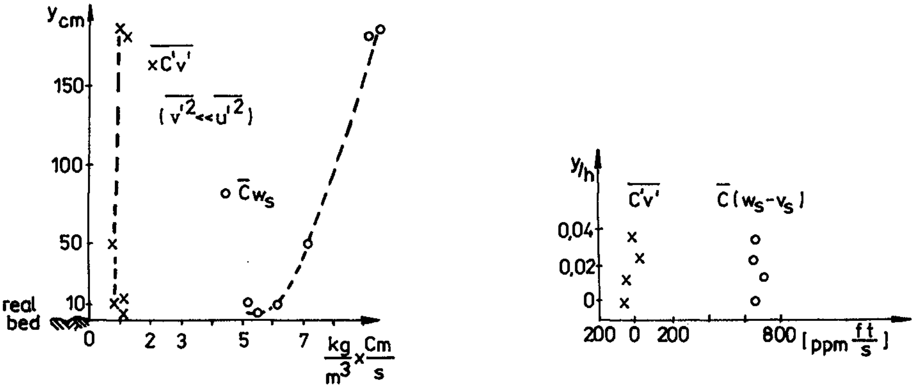

Fig. 10 Correlations $\overline{C'v'}$ for Random Waves (left) and Regular Waves (right, after Kennedy & Locher, 1972)

The Author also conducted other field studies, in particular a very extensive year-long coastal expedition in Senegal. Since they incorporate some other aspects as well, they are discussed in the next chapter.

3. SCHEMATIZATION OF SUSPENDED LOAD PROFILES

3.1. Gross Estimates of K

Chapter 1 and 2 show that vertical profiles of sediment concentration can be described in three layers, for which the exponents $2b$ in $C \sim C_0 \exp(-2by/h)$ can be postulated in various forms, depending on dispersion-controlling mechanisms.

A considerable bulk of data has been collected, which makes possible validation of the concept and formulae put forward. The data includes many alien sources, such as those mentioned above, e.g. some more recent by Skafel and Krishnappan (1984) Antsyferov and Kosyan (1986), and the Author's own data for the Baltic Sea, the Black Sea and particularly those from the coastal project off St. Louis, Senegal in 1980...81 (Zeidler, 1982 and Skaja & Zeidler, 1982). The results of the latter embody 98 vertical profiles of sediments concentration, ranging from instantaneous to averaged long-term ones, such as those exemplified in Fig. 11.

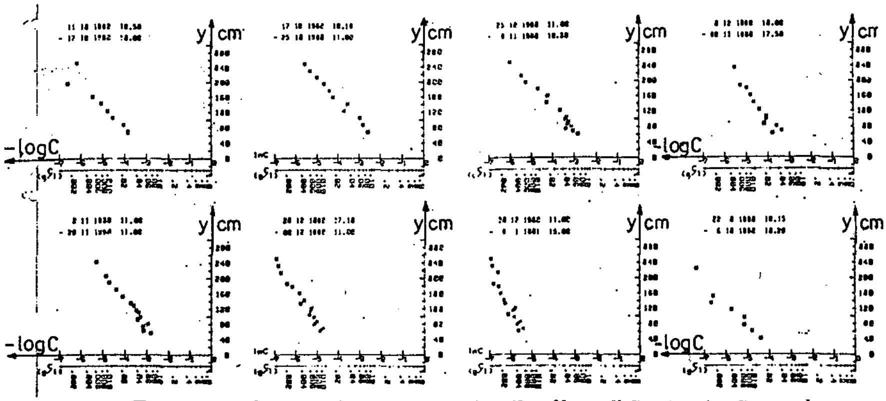

Fig. 11 Examples of Author's Concentration Profiles off St. Louis, Senegal

The available concentration profiles are exponential, so that their slopes can be identified with $2b = w_s h / 2\overline{K}_y$. The following tentative conclusions may be drawn from the regression analysis attempted for $2b$.

1. In wave-dominated areas of motion, with $\widetilde{K} \gg K$ one has

$$2b \simeq 4w_s \frac{hT}{H^2}; \quad \sigma_{2b} \simeq 1\frac{w_s Th}{H^2} \quad (R^2 \simeq 0.7) \tag{23.1}$$

2. In wind wave-induced dispersion

$$< \widetilde{K} > \simeq 2 \cdots \widetilde{K}_{\text{significant}} \qquad (\widetilde{R} \simeq 0.6) \tag{23.2}$$

3. In bed shear-controlled areas (within surf zone), with $K \gg \widetilde{K}$, one may postulate

$$2b \simeq 40\frac{w_s}{u_*} + \quad +0(h/l) \quad (R^2 \simeq 0.6) \tag{23.3}$$

Other dispersion mechanisms can be dealt with similarly.

Extensive studies under CMEA programmes, in particular Lubiatowo'74, Lubiatowo'76, Kamchiya'77, Kamchiya'79, and other measurements in the two coastal research stations (Polish Lubiatowo and Bulgarian Kamchiya, or Shorpilovtsy) have shown that the layered structure of exponential concentration profiles persists everywhere in the coastal zone, both inshore and offshore. The profiles may be further schematized by attributing, to the nearbed and central layer, distinctly different slopes of the exponential branches (which are straight lines in the semilog plot, cf. Fig. 3a). The slope is relatively mild in the offshore zone, becomes very steep in the breaking zone (where the two layers practically merge), and is again milder (particularly in the nearbed layer) in the inshore zone.

3.2. Examples of Cross-Shore Distributions of Suspended Sediment

In engineering computations, it is equally important to know both b and Q_{02}

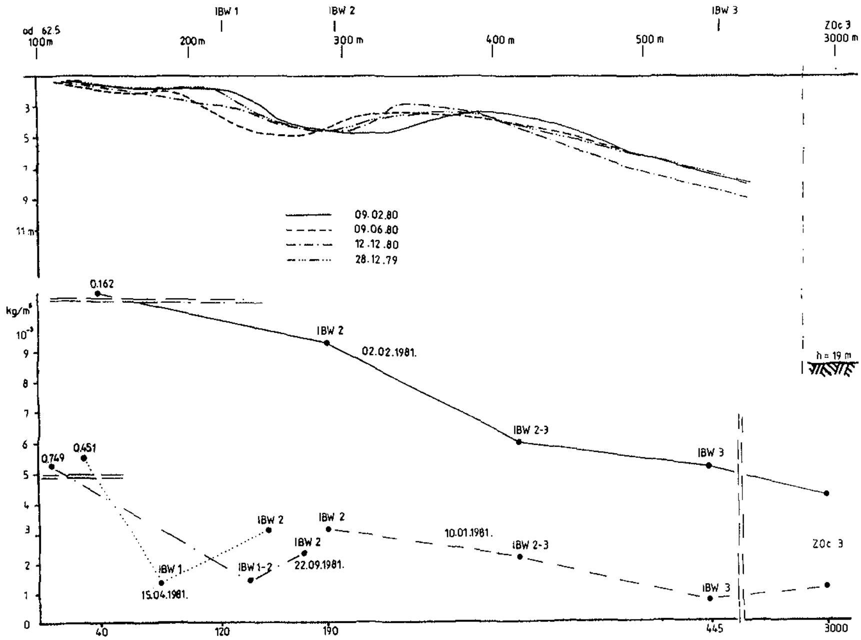

Fig. 12 Examples of Author's Cross-Shore Profiles of Suspended Mass (bottom) and Bed Topography (top) off St. Louis, Senegal

in the exponential profile $C = Q_{02}\exp(-2by/h)$. While b shows how much of the water depth is laden with sediment (or its practically important quantities), it is Q_{02} which determines the absolute magnitude of saturation with sediment. Vertical profiles of sediment concentration, such as those depicted in Fig. 11 not only provide figures for the exponent b but also yield estimates for Q_{02} and the suspended load. The data collected under the programmes mentioned in this paper gives insight into absolute magnitudes and notably the cross-shore distribution of suspended load, the latter being found through obvious integration of the concentration profile over the entire depth of water, with proper account for the layered structure of the C-profile.

Illustrated in Fig. 12 are some examples for the situations encountered off St. Louis, Senegal. It is interesting to note high figures in the zone of ultimate breaking and in the swash zone, where permanent turbidity was recorded, on most occasions, due to considerable turbulence. Although some correlations between Q_{02} and the coastal climate have already been formulated, a lot of work remains to be done before reliable estimates of b and Q_{02} will have been available for all possible coastal situations.

CLOSING REMARKS

The theoretical findings presented in this paper, supported by vast experimental evidence, point to the exponential profile as simple and well substantiated representation of the vertical distribution of suspended sediment concentration. The exponent has been correlated with external factors but more efforts are required for better quantitative description of coastal sediment fields in absolute physical terms. – A concise summary is provided in Abstract.

ACKNOWLEDGEMENTS

This study has been sponsored under the Polish Academy of Sciences' programme CPBP 02.12.2, which is gratefully acknowledged.

REFERENCES

1. Antsyferov S. M., Kosyan R. D., (1986), *Suspended Sediment in the Upper Shelf* (in Russian), Nauka, Moscow, 224p.

2. Homma M., Horikawa K., (1962), *A laboratory study* on *suspended sediment due to wave action*, Proceed. X Conf. IAHR, London, Vol. 1, 213-221.

3. Homma M., Horikawa K., Kajima R., (1965), *A study of suspended sediment due to wave action*, Coastal Eng. in Japan, Vol. 8, 85-103.

4. Kennedy J. F., Locher F. A., (1972), *Sediment suspension by water waves*, in *Waves on Beaches*, Acad. Press, 249-295.

5. Keremedchiyev S. D., (1982), *Morphologic analysis of equilibrium profile and wave parameters in laboratory conditions*, (in Bulgarian), Okeanologia (Sofia), No 9, 54-63.

6. Nguyen V. G. and Zeidler R., (1982), *Turbulent Diffusion of Suspended Sediment in Open-Channel Flow*, PRACE IBW PAN, Gdańsk, 160p.

7. Sawicki J. M., (1988), *Analysis of spatial models of turbulence*, Archiwum Hydrotechniki (in press).

8. Skafel M. G., Krishnappan B. G., (1984), *Suspended sediment distribution in wave field*, Journal Waterway ... Ocean Engineering, Vol. 110, No. 2, 215-230.

9. Skaja M., Zeidler R. B., (1982), *Longshore sediment transport rate*, 18th Intern. Conf. Coastal Eng. Abstracts, ASCE.

10. Stive M. J. F., Wind H. G., (1986), *Cross-shore mean flow in the surf zone*, Coastal Engineering Vol. 10, No. 4, 325-340.

11. Taggart W. C., Yermoli C. A., Montes S., Ippen A. T., (1972), *Effects of sediment size and gradation on concentration profiles in turbulent flow*, Rep. No. 152, Parsons Lab., Mass. Inst. Techn., 153p.

12. Yaglom A. M., (1976), *Semi-empirical equations of turbulent diffusion in boundary layers*, Fluid Dynamics Transactions, Vol. 7, p. I, IPPT PAN Warsaw, 99-144.

13. Zeidler R. B., (1972), *Nearbed turbulence under waves* (in Polish), Archiwum Hydrotechniki, Vol. XVIII, No. 2, 147-166.

14. Zeidler R. B., (1982), *Yearly measurements off St. Louis, Senegal*, 18th Intern. Conf. Coastal Eng. Abstracts, ASCE.

15. Zeidler R. B., (1987a), *Suspended sediment transport and beach profile evolution*, Discussion, Journal Waterway ... Ocean Eng., ASCE, Vol. 113, no. 1, 89-95.

16. Zeidler R. B., (1987b), *Concentration and transport rate of suspended sediment in marine and fluvial environments*, Euromech 215, Univ. Genoa, Ext. Abstr., 96-100.